Traffic 2005; **6:** 374–385
Blackwell Munksgaard

doi: 10.1111/j.1600-0854.2005.00282.x

Dissection of Membrane Dynamics of the ARF-Guanine Nucleotide Exchange Factor GBF1

Tomasz Szul, Rafael Garcia-Mata[1], Elizabeth Brandon, Svetlana Shestopal, Cecilia Alvarez[2] and Elizabeth Sztul*

Department of Cell Biology, University of Alabama at Birmingham, Birmingham, AL 35924, USA
**Corresponding author: Elizabeth Sztul, esztul@uab.edu*

ADP-ribosylation factor (ARF)-facilitated recruitment of COP I to membranes is required for secretory traffic. The guanine nucleotide exchange factor GBF1 activates ARF and regulates ARF/COP I dynamics at the endoplasmic reticulum (ER)–Golgi interface. Like ARF and coatomer, GBF1 peripherally associates with membranes. ADP-ribosylation factor and coatomer have been shown to rapidly cycle between membranes and cytosol, but the membrane dynamics of GBF1 are unknown. Here, we used fluorescence recovery after photobleaching to characterize the behavior of GFP-tagged GBF1. We report that GBF1 rapidly cycles between membranes and the cytosol ($t_{1/2}$ is approximately 17 ± 1 seconds). GBF1 cycles faster than GFP-tagged ARF, suggesting that in each round of association/dissociation, GBF1 catalyzes a single event of ARF activation, and that the activated ARF remains on membrane after GBF1 dissociation. Using three different approaches [expression of an inactive (E794K) GBF1 mutant, expression of the ARF1 (T31N) mutant with decreased affinity for GTP and Brefeldin A treatment], we show that GBF1 is stabilized on membranes when in a complex with ARF–GDP. GBF1 dissociation from ARF and membranes is triggered by its catalytic activity, i.e. the displacement of GDP and the subsequent binding of GTP to ARF. Our findings imply that continuous cycles of recruitment and dissociation of GBF1 to membranes are required for sustained ARF activation and COP I recruitment that underlies ER-Golgi traffic.

Key words: ARF GTPase, Brefeldin A, COP I, fluorescence recovery after photobleaching, GBF1, guanine nucleotide exchange factor

Received 6 January 2005, revised and accepted for publication 31 January 2005, published on-line 9 March 2005

Membrane traffic requires the sorting of proteins into transport intermediates. This process is mediated by the selective recruitment of specific coats that form two-dimensional scaffolds for clustering proteins destined for transport (1). The COP I coat functions within the Golgi and at transport intermediates (often called vesicular-tubular clusters or VTCs) positioned between the endoplasmic reticulum (ER) and the Golgi. COP I coat is recruited to membranes by a small GTPase of the Ras superfamily, the ADP-ribosylation factor (ARF). ADP-ribosylation factors are ubiquitous among eukaryotes and are essential for cell survival (2–6).

ADP-ribosylation factors, like other GTPases, cycle between an inactive GDP-bound and an active GTP-bound state (3). Exchange of GTP for GDP induces a conformational change that allows the GTPase to interact with high affinity with several downstream effectors, most notably COP I, and help regulate protein sorting and the formation of transport intermediates. The cellular activity of ARFs is determined by the ratio of their GTP/GDP-bound forms. This ratio is tightly regulated by two distinct families of proteins: guanine nucleotide exchange factors (GEFs) and the GTPase-activating proteins or GAPs. Guanine nucleotide exchange factors activate ARF proteins by catalyzing the exchange of GDP for GTP, therefore increasing the levels of the GTP-bound ARF forms in the cell. Conversely, ARF-GAPs negatively regulate GTPase function by stimulating GTP hydrolysis, therefore increasing the levels of the GDP-bound state.

ADP-ribosylation factor-GEFs comprise a family of GEFs that share a highly conserved 200-amino acid catalytic domain (initially identified in the yeast protein Sec7p) termed the Sec7 domain (7,8). Sec7 domain proteins are subdivided into two major classes based on size and sequence similarities. The small Sec7 domain GEFs (<100 kDa) have been found only in higher eukaryotes and have no orthologs in *Saccharomyces cerevisiae*, suggesting a function specific to metazoans. The large Sec7 domain GEFs (>100 kDa) have orthologs in all eukaryotes examined, indicating an earlier origin and an evolutionary conserved role.

Several lines of evidence suggest that one of the large ARF-GEFs, GBF1, is responsible for the regulation of ARF activity and COP I recruitment at the ER–Golgi interface. GBF1 localizes to the Golgi, VTCs, and to a lesser extent, the ER (9–13). GBF1 has been implicated in COP I recruitment at the ER–Golgi interface, based on the findings that the overexpression of GBF1 prevents Brefeldin A (BFA)-induced COP I dissociation *in vivo* (10). In addition, the expression of a dominant negative inactive mutant of GBF1 inhibits COP I recruitment and inhibits ER to Golgi traffic *in vivo* (9).

[1]Present address: Department of Cell and Developmental Biology, University of North Carolina, Chapel Hill, NC 27599, USA.
[2]Present address: Dpto. de Bioquimica Clinica, Fac. Ciencias Quimicas, Ciudad Universitaria, Cordoba CP.5000, Argentina.

The recruitment of COP I to membranes appears to be a stochastic process, and COP I undergoes rapid cycles of binding to and dissociation from the membranes (14–16). The dissociation of COP I is linked to the rapid cycling of ARF and appears to be triggered by GTP hydrolysis by the ARF (14–16). The recruitment of COP I and ARF to membranes despite their constant dissociation implies that the machinery that initiates the coating cascade, i.e. GBF1, must also associate with membranes. However, the mechanisms that regulate GBF1 residency on membranes are unknown.

Herein, we report that GBF1 rapidly cycles between cytosol and membranes and that GBF1 cycling is influenced by its catalytic activity. Our data indicate that GBF1–ARF–GDP complexes are stably associated with membranes. GBF1 dissociates from the ARF and from the membrane after the exchange of GTP for GDP has been completed. GBF1 dissociation is independent from the fate of the activated ARF–GTP, which remains on membranes where it interacts with its effectors. GBF1 is therefore critical for the spatially and temporally restricted activation of ARFs, but does not appear to participate in downstream events mediated by ARF–GTP. Our description of GBF1 behavior provides a model for investigating the behavior or other cellular GEFs.

Results

Cycling kinetics of GBF1

GBF1 is recovered as a soluble cytoplasmic protein after cell fractionation (10,12). Other traffic factors, such as εCOP, ARF1, or Sar1p, that fractionate as soluble proteins have been shown previously to rapidly cycle on and off membranes, presumably to continuously generate new, potential transport sites (15–17). Their rate of binding and dissociation from membranes has been determined using fluorescence recovery after photobleaching (FRAP) of GFP-tagged proteins.

We used FRAP to monitor the dynamic exchange of GBF1 on membranes. GBF1 was tagged at the N-terminus with GFP and expressed in HeLa cells. Like the endogenous protein, GBF1-GFP localizes predominantly to the Golgi and to peripheral sites (Figure 1A and data not shown). In addition, GBF1-GFP fractionates in a manner analogous to endogenous GBF1 after cell homogenization and differential centrifugation (Figure 5H).

For FRAP studies, a section of the Golgi was photobleached, and the recovery of GBF1-GFP fluorescence within the bleached region was quantitated and fit to a first-order equation to determine the rate of recovery of GBF1-GFP in the bleached area. If we assume that the dissociation of GBF1-GFP from membranes is the rate-limiting step in the on/off cycle, then the rate of recovery of fluorescence is directly related to a rate of the dissociation of the protein from the membranes [previous studies have shown that the rate of diffusion of soluble proteins ($t_{1/2}$ is approximately 3 seconds) is not rate-limiting under those conditions]. As shown in Figure 1C, the fluorescence level was approximately 38% of the starting fluorescence intensity at 6 seconds after bleaching (the image acquisition in our studies takes approximately 6 seconds). GBF1 fluorescence recovered rapidly over the next 30 seconds, with >80% recovery reached in <40 seconds after bleaching (Figure 1E). Approximately 38% value obtained at the first time-point may be due to incomplete bleaching of the sample or to rapid recovery within the 6-second interval required for image acquisition. Fluorescence recovery after photobleaching on fixed cells was performed to differentiate these scenarios. The first postbleached image in paraformaldehyde-fixed cells shows 12% fluorescence intensity, suggesting that the bleaching conditions bleach >88% of molecules at time 0 (Figure 1E). This suggests that approximately 38% value observed in live cells represents a combination of some unbleached GBF1-GFP (approximately 12%) and recovery that occurs during the first 6 seconds (approximately 24%). The approximate $t_{1/2}$ of fluorescence recovery for GBF1 from this and analogous experiments is approximately 17 ± 1 seconds.

The fluorescence recovery may be due to the delivery of GBF1 to the bleached area on anterograde transport intermediates coming from the ER. We therefore explored GBF1-GFP recovery in cells treated with nocodazole (to inhibit the movement of transport intermediates). GBF1-GFP was imaged in cells incubated on ice to depolymerize microtubules and then supplemented with nocodazole to prevent microtubule polymerization during the subsequent imaging. Disruption of microtubules leads to the disappearance of the perinuclear Golgi, and the relocation of Golgi proteins to peripheral Golgi mini-stacks (18–20). Like other Golgi proteins, GBF1-GFP is detected in peripheral structures in nocodazole-treated cells (Figure 1B). The FRAP time of GBF1-GFP within the disrupted structures is very similar to that observed in untreated cells with $t_{1/2}$ of recovery of 18 ± 0.5 seconds (Figure 1D,E). This suggests that the rapid exchange of GBF1 on Golgi membranes is independent of microtubule-mediated anterograde traffic and intact Golgi morphology.

The $t_{1/2}$ of approximately 17 seconds for GBF1 recovery is similar to the reported $t_{1/2}$ (approximately 15 seconds) for ARF1 recovery determined by FRAP (15,16). We measured the dynamics of ARF-GFP in our system to directly compare GBF1 and ARF cycling. ARF1-GFP FRAP shows slower recovery than that of GBF1-GFP, with $t_{1/2}$ of 24 ± 2.7 seconds (Figure 1E). We expect that the slower cycling of ARF-GFP in our experiments may be due to slightly lower temperature of the imaging stage of our microscope setup.

Cycling kinetics of GBF1 are modulated by its nucleotide exchange activity

We have previously generated an inactive mutant of GBF1, E794K (9). The glutamic acid to lysine substitution within

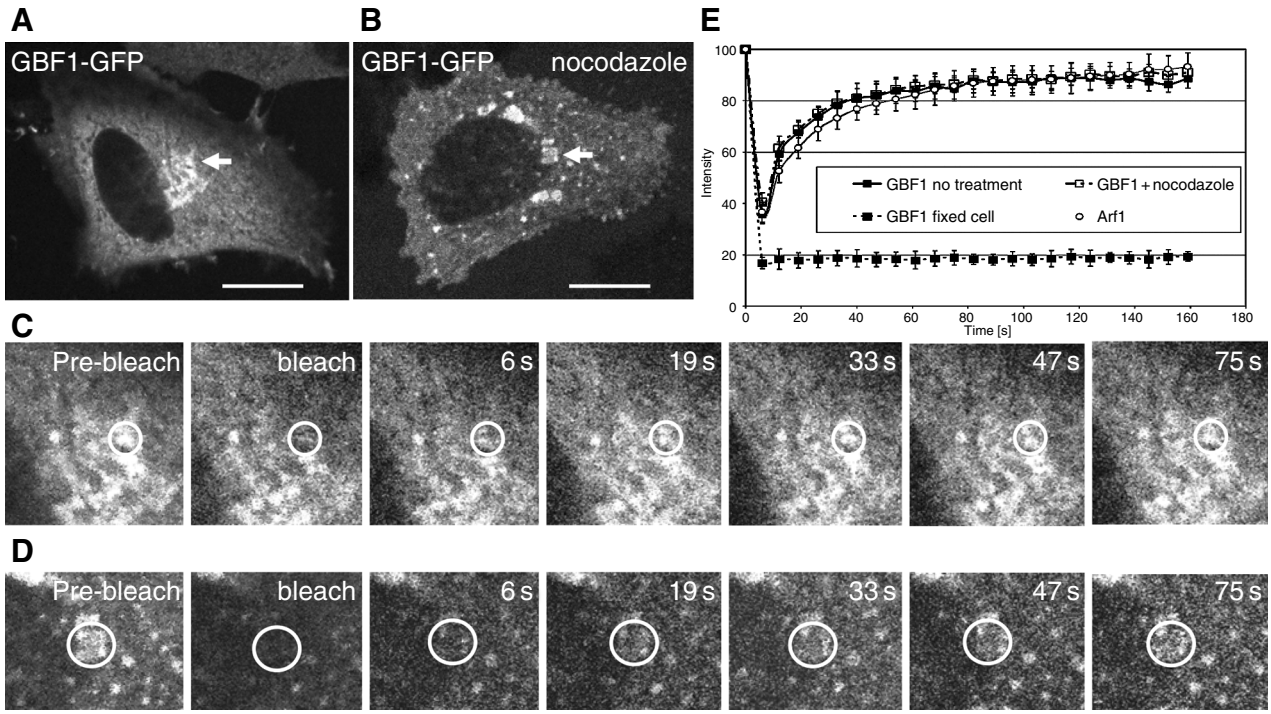

Figure 1: Cycling kinetics of GBF1-GFP. HeLa cells were transfected with GBF1-GFP and 16 h later, either imaged directly or treated with nocodazole before imaging. A) GBF1-GFP localizes to the Golgi in an untreated cell. The arrow points to a region subjected to fluorescence recovery after photobleaching (FRAP) in C. B) GBF1-GFP localizes to peripheral structures in a cell incubated with nocodazole. The arrow points to a region subjected to FRAP in D. C) A gallery of images showing prebleach, bleach and recovery of GBF1-GFP fluorescence in the Golgi. D) A gallery of images showing prebleach, bleach and recovery of GBF1-GFP fluorescence in the peripheral structures. E) Recovery graphs calculated from images analogous to those in C and D; $n = 5$ (bars represent SD). Half-life of GBF1-GFP in control cells and in cells treated with nocodazole is approximately 17 ± 1 and 18 ± 0.5 seconds, respectively. An analogous experiment was performed on ARF1-GFP in control cells and on GBF1-GFP in fixed cells. Their fluorescence recovery graphs are included in E. Bars represent 16 μm.

the catalytic Sec7 domain abolishes the nucleotide exchange activity of all tested ARF-GEFs. The mutant GEFs bind ARF–GDP, but do not catalyze GDP displacement (21). The phenotype of cells expressing E794K is analogous to cells treated with BFA: COP I dissociates from membranes, and Golgi proteins relocate to the ER or to peripheral sites adjacent to ER exit sites (9). The E794K mutant localizes to such peripheral sites (Figure 2A). Previous time-lapse imaging showed that the E794K-GFP-labeled structures are relatively immobile and that they are relatively short-lived and disappear with a $t_{1/2}$ of <10 min (9). Often, new E794K-GFP-labeled structures form at the same site where a structure was seen disappearing.

Fluorescence recovery after photobleaching analysis of E794K-GFP on peripheral structures was performed. The fluorescence recovers with a $t_{1/2}$ of 53 ± 12.2 seconds (Figure 2B,C), significantly slower than $t_{1/2}$ of approximately 17 ± 1 seconds seen for wild-type GBF1-GFP. It takes almost 3 min to recover approximately 80% of E794K fluorescence, in contrast to <40 seconds for wild-type GBF1. Furthermore, there is a marked difference in the mobile fractions of GBF1 and E794K: approximately 90% of GBF1 appears mobile while only approximately 60% of E794K is mobile (compare percentage recovery of GBF1 and E794K 1 min after photobleaching). These findings indicate that the exchange activity modulates GBF1 cycling kinetics and that the E794K-GFP (predicted to be in a complex with ARF–GDP) is stabilized in its mobility relative to a wild-type GBF1-GFP. In agreement with this prediction, ARF colocalizes with E794K in the peripheral structures (Figure 2D). The E794K stabilization suggests that the rate-limiting step in GBF1 cycling on/off membranes is linked to its catalytic activity. This conclusion supports a model in which a single cycle of GBF1 binding to and release from membranes may result in the activation of a single ARF molecule.

Cycling kinetics of GBF1 in cells expressing ARF mutants

GBF1 dissociation appears to be regulated by its exchange activity. The dissociation may occur when GBF1 displaces GDP, or later, when GTP binds to the ARF. This was explored by examining GBF1-GFP behavior in cells overexpressing the dominant negative T31N or the constitutively

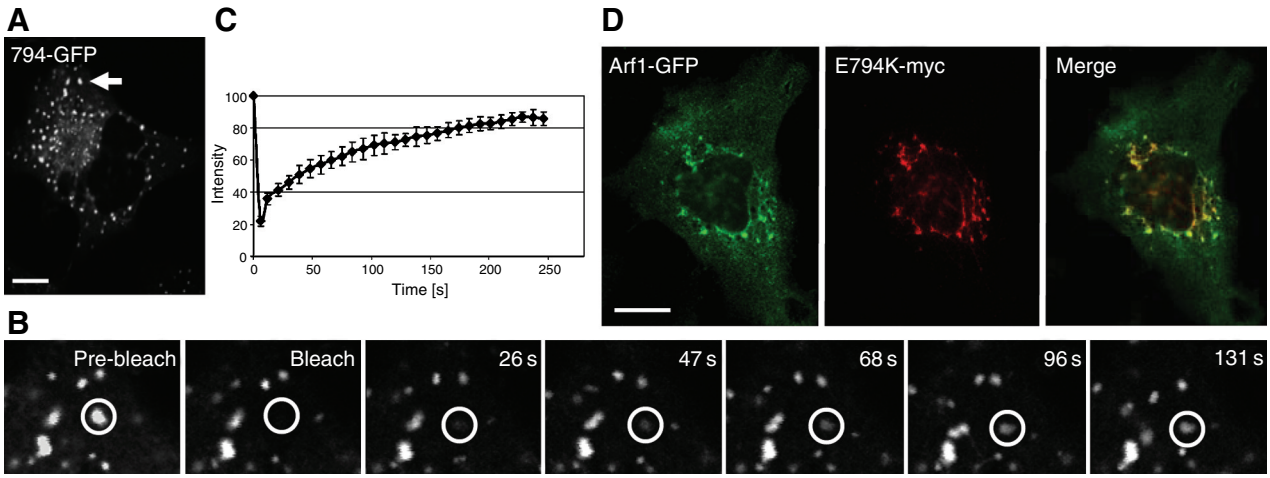

Figure 2: Cycling kinetics of inactive E794K mutant of GBF1. A–C) HeLa cells were transfected with E794K-GFP and 16 h later subjected to fluorescence recovery after photobleaching (FRAP) analysis. A) E794K-GFP localizes to peripheral structures. The arrow points to a region subjected to FRAP in B. B) A gallery of images showing prebleach, bleach and recovery of E794K-GFP fluorescence in the peripheral structures. C) Recovery graph calculated from images analogous to those in B; $n = 5$ (bars represent SD). Half-life of E794K-GFP is approximately 53 ± 12.2 seconds. D) HeLa cells were cotransfected with E794K-myc and ARF1-GFP and processed for double-label immunofluorescence with anti-GFP and anti-myc antibodies. Arf1-GFP and E794K-myc colocalize in peripheral structures. Bars represent 16 μm.

active Q71I mutants of ARF1 (22). ARF1 has been shown to support the GTP-dependent association of COP I with membranes *in vitro* (5), and *in vivo* observations suggest that GBF1 can act on ARF1 (12).

The ARF1-T31N mutant has reduced affinity for GTP, and following GDP displacement, it remains 'nucleotide-free' for longer than wild-type ARF. Like BFA treatment or expression of the dominant-negative E794K mutant of GBF1, expression of ARF1-T31N causes the release of COP I into the cytosol (23) and Golgi disassembly (9). In cells expressing T31N, some Golgi proteins relocate to the ER, while others, exemplified by GBF1, relocate to peripheral compartments adjacent to ER exit sites (Figures 3B and 4A). GBF1 colocalizes with T31N in the peripheral sites (Figure 3B, insert), but the majority of T31N appear to be more diffusely distributed. This is consistent with previous findings suggesting that ARF–GDP can associate with membranes prior to being activated by a GEF (24).

Fluorescence recovery after photobleaching of GBF1-GFP in cells expressing the ARF1-T31N mutant shows slower recovery time, with $t_{1/2}$ of approximately 45 ± 5.7 seconds (Figure 4C,E,F). It takes more than 2 min to recover approximately 80% of GBF1 fluorescence in cells expressing T31N, in contrast to <40 seconds in control cells. In addition, there is a marked difference in the mobile fractions of GBF1 in control and ARF1-T31N-expressing cells: approximately 90% of GBF1 appears mobile in control cells, while only approximately 60% of GBF1 is mobile in cells expressing the ARF mutant (compare percentage recovery in control and ARF1-T31N cells 1 min after photobleaching). This suggests that GBF1 binds to ARF1-T31N in cells and as a result is stabilized on membranes when GTP binding to ARF is impaired. GTP binding to ARF would thus appear to be the release trigger, both for the dissociation of GBF1 from the GTPase and for the release of GBF1 from the membrane. A prediction would be that events downstream of GTP binding would not influence GBF1 dissociation. This was explored by using the ARF-Q71I mutant.

ARF1-Q71I undergoes normal GDP/GTP exchange, but is defective in GTP hydrolysis and persists in the GTP-bound state longer than wild-type ARF. Expression of ARF1-Q71I results in a prolonged ARF1 activation and promotes binding of coatomer to the Golgi (25, 51). Expression of ARF1-Q71I leads to increase in Golgi size in some cells and to the appearance of punctate peripheral structures (Figure 3C). GBF1-GFP colocalizes with ARF-Q71I in the enlarged Golgi and in the peripheral structures (Figure 3C). The changes in morphology are not due to cotransfection, as cotransfection of GBF1-GFP and wild-type ARF does not alter Golgi morphology (Figure 3A).

Fluorescence recovery after photobleaching of GBF1-GFP in cells expressing the ARF1-Q71I mutant is analogous to control cells, with $t_{1/2}$ of approximately 18 ± 0.8 seconds (Figure 4B,D,E). The percentage mobile fraction (approximately 90%) is also analogous to that seen in control cells. This indicates that the addition to cells of ARF1-Q71I that is predominantly in the GTP-bound form does not alter the normal cycling time of GBF1-GFP. This is consistent with *in vitro* findings that GEFs have low affinity for activated GTPases (21,26–28). Our findings suggest a model in

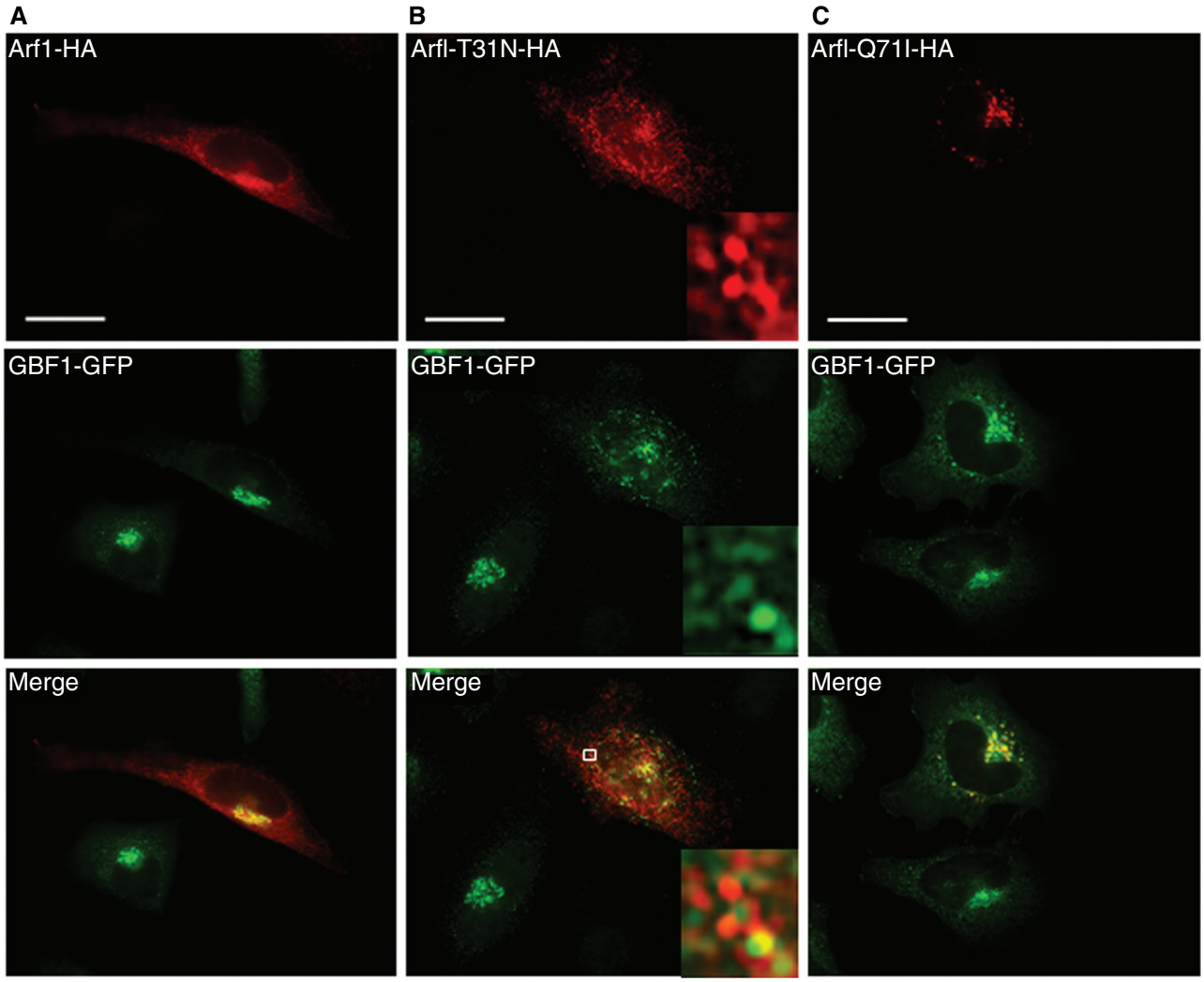

Figure 3: Localization of GBF1-GFP in cells expressing ADP-ribosylation factor (ARF) mutants. HeLa cells were cotransfected with GBF1-GFP and either wild-type ARF1, the T31N, or the Q71I mutant of ARF1. All ARF constructs are HA tagged. Twenty-four hours later, cells were processed for double-label immunofluorescence with anti-GFP and anti-HA antibodies. A) GBF1-GFP and wild-type ARF1 colocalize in a morphologically normal Golgi. B) GBF1-GFP localizes to disperse structures in a cell expressing the T31N ARF mutant. Insert shows partial colocalization of ARF1-T31N and GBF1 in punctate peripheral structures. C) GBF1-GFP and ARF1-Q71I colocalize in an enlarged Golgi and in dispersed punctate structures. Bars represent 16 μm.

which GBF1 cycling kinetics are independent of ARF–GTP-mediated coat recruitment.

Cycling kinetics of GBF1 in BFA-treated cells

The findings that GBF1 appears stabilized on membranes when complexed with ARF–GDP led us to test GBF1 behavior in cells treated with BFA. Brefeldin A is known to stabilize a ternary complex of ARF–GDP and a GEF and prevent GDP displacement.

Endogenous GBF1 relocates to the ER in BFA-treated cells (29). In agreement, GBF1-GFP shows a diffuse reticular pattern after BFA treatment (Figure 5A). GBF1 behavior is analogous to that of giantin. GBF1 does not appear to colocalize with GM130, which relocates to peripheral structures adjacent to ER exit sites.

Fluorescence recovery after photobleaching of GBF1-GFP in BFA-treated cells shows delayed recovery that reaches a maximum of approximately 70% after more than two and a half minutes, in contrast to >80% recovery in 40 seconds in control cells (Figure 5C,E,G). Two alternative models may explain this behavior. First, GBF1-GFP continues to exchange between the cytosol and the ER membrane, albeit at a reduced rate. Alternatively, GBF1-GFP remains associated with the ER membrane, and the observed recovery reflects its mobility within the plane of

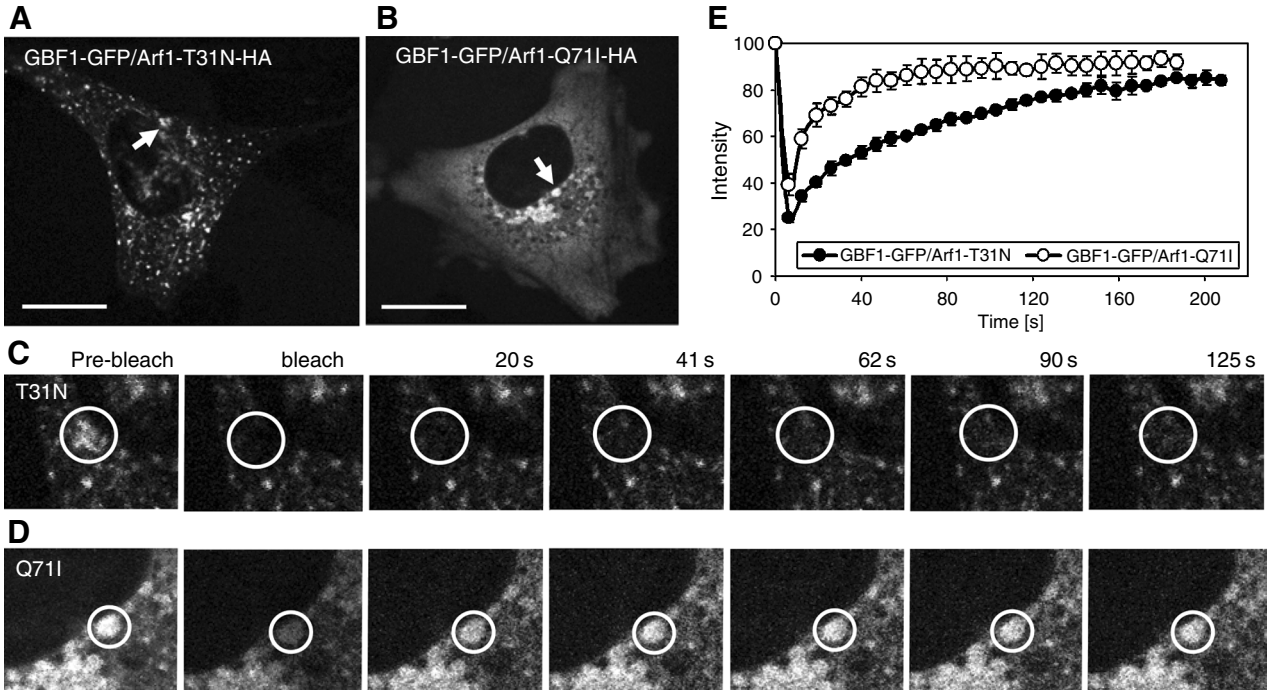

Figure 4: Fluorescence recovery after photobleaching (FRAP) of GBF1-GFP in cells expressing ARF1-T31N or ARF1-Q71I. HeLa cells were cotransfected with GBF1-GFP and either ARF1-T31N or ARF1-Q71I. Sixteen hours later, cells showing altered Golgi morphology (altered GBF1-GFP localization) were subjected to FRAP analysis. A) GBF1-GFP localizes to peripheral structures in a cell expressing the ARF1-T31N mutant. The arrow points to a region subjected to FRAP in C. B) GBF1-GFP localizes to a punctate structure in a cell expressing the ARF1-Q71I mutant. The arrow points to a region subjected to FRAP in D. C) A gallery of images showing prebleach, bleach and recovery of GBF1-GFP fluorescence in peripheral sites in a cell expressing the ARF1-T31N mutant. D) A gallery of images showing prebleach, bleach and recovery of GBF1-GFP fluorescence in punctate structures in a cell expressing the ARF1-Q71I mutant. E) Recovery graphs calculated from images analogous to those in C and D; $n = 5$ in each case (bars represent SD). Half-life of GBF1-GFP in cells expressing the ARF1-T31N mutant is 45 ± 5.7 seconds when compared with half-life of 18 ± 0.8 seconds in cells expressing the ARF1-Q71I mutant. Bars represent 16 μm.

the membrane. To distinguish between these possibilities, we explored the behavior of GBF1-GFP in cells first treated with nocodazole and then with BFA. The disruption of microtubules prevents the collapse of the Golgi to the ER during the subsequent BFA treatment. In nocodazole/BFA-treated cells, COP I dissociates from the membranes, but Golgi proteins do not redistribute to the ER (20,30). Instead, Golgi proteins localize to peripheral punctate structures. In cells treated with nocodazole and BFA, GM130, giantin and GBF1-GFP colocalize in the peripheral structures (Figure 5B).

Fluorescence recovery after photobleaching of GBF1-GFP in cells treated with nocodazole/BFA shows decreased recovery that reaches a maximum of only approximately 55% after approximately 4 min (Figure 5D,F,G). The $t_{1/2}$ of 31 seconds is similar to that seen in the control cells. However, the incomplete recovery of GBF1 indicates a significant (approximately 60%) immobile fraction and reveals that GBF1 is stabilized on membranes in BFA-treated cells.

This result was further validated by fractionation. In control cells transfected with GBF1-GFP, the majority (approximately 80%) of GBF1-GFP and of endogenous GBF1 is recovered in the cytoplasmic fraction (Figure 5H, lane 3). Similarly, in cells treated only with nocodazole, GBF1 and GBF1-GFP are predominantly cytosolic (Figure 5H, lane 9). In contrast, in cells treated with BFA, GBF1-GFP and endogenous GBF1 are preferentially (approximately 90%) recovered with membranes (Figure 5H, lane 5). The recovery of calnexin exclusively in the membrane fractions (lanes 2, 5 and 8) and the recovery of β-tubulin exclusively in the cytosolic fractions (lanes 3, 6 and 9) confirm the efficacy of fractionation. These data indicate that GBF1-GFP is stabilized on membranes in BFA-treated cells.

Discussion

ADP-ribosylation factor-mediated recruitment of COP I to membranes plays a central role in transport between the ER and the Golgi. The activation of ARF at the ER–Golgi interface requires the GEF activity of GBF1. Although the transient nature of ARF and COP I association with membranes has been documented, the dynamics of GBF1 have not been reported. Here, we demonstrate that GBF1

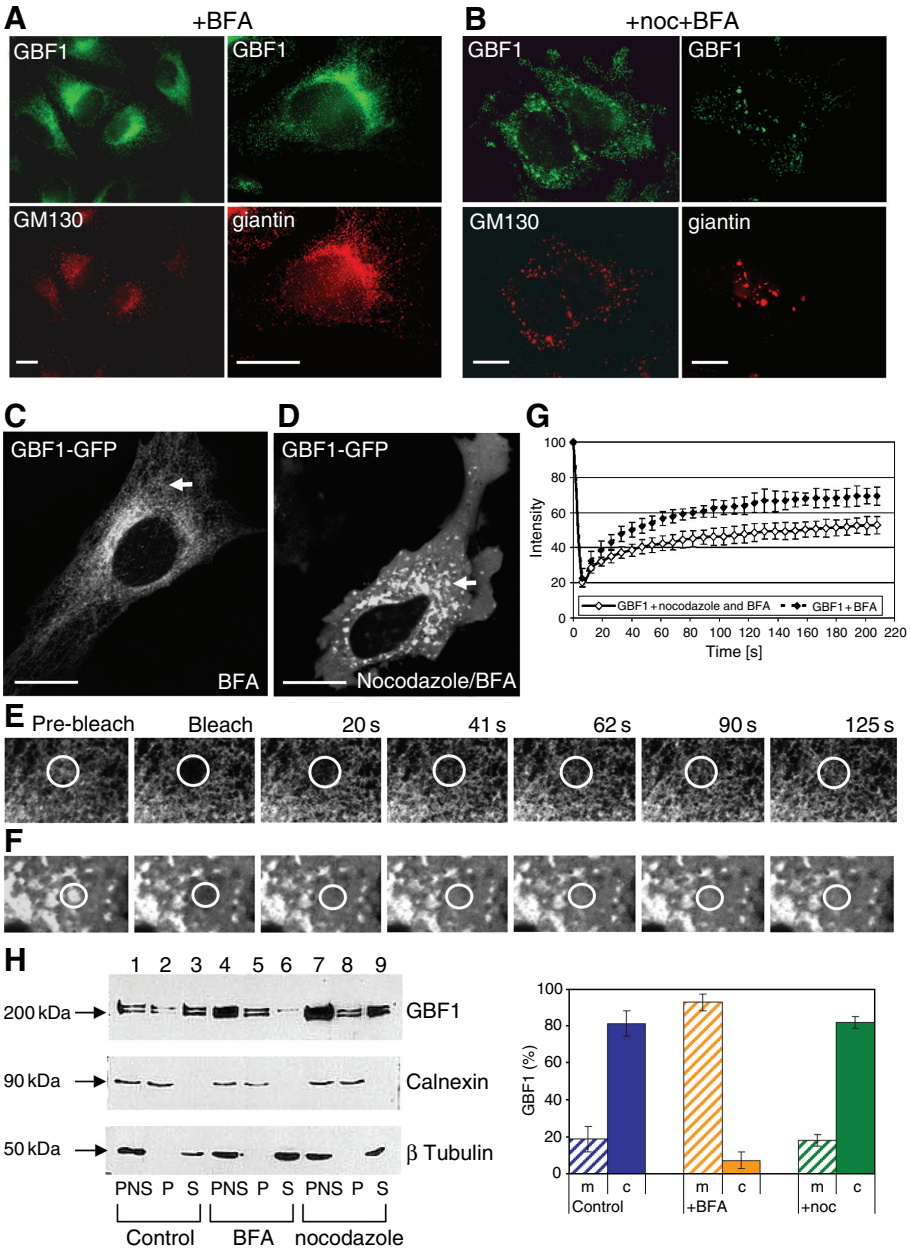

Figure 5: Fluorescence recovery after photobleaching (FRAP) of GBF1-GFP in cells treated with Brefeldin A (BFA). A and B HeLa cells were treated with BFA or with nocodazole followed by BFA. Cells were either processed for double-label immunofluorescence with anti-GBF1 antibodies and either anti-GM130 or anti-giantin antibodies. A) GBF1-GFP localizes to the endoplasmic reticulum (ER) in cells treated with BFA. It behaves like giantin, which also relocates to the ER and unlike GM130 which localizes to punctate structures adjacent to ER exit sites. B) GBF1-GFP colocalizes with giantin and GM130 in dispersed structures in cells treated with nocodazole followed by BFA. C–H) HeLa cells were transfected with GBF1-GFP for 16 h, and then treated with BFA, or with nocodazole followed by BFA. Cells were then subjected to FRAP analysis. C) GBF1-GFP relocates to ER after BFA treatment. The arrow points to a region subjected to FRAP in E. D) GBF1-GFP localizes to disperse structures in a cell incubated with nocodazole and BFA. The arrow points to a region subjected to FRAP in F. E) A gallery of images showing prebleach, bleach and recovery of GBF1-GFP fluorescence within the ER. F) A gallery of images showing prebleach, bleach and recovery of GBF1-GFP fluorescence in dispersed structures. G) Recovery graphs calculated from images analogous to those in C and D; $n = 6$ in each case (bars represent SD). H) HeLa cells were transfected with GBF1-GFP for 16 h, and then treated with BFA, nocodazole, or nocodazole followed by BFA. Cells were homogenized and subjected to differential centrifugation. Following fractionation, equivalent amount of the PNS, cytosolic and membrane fractions were resolved by SDS–PAGE and Western blotted with anti-GBF1 antibodies. The same nitrocellulose filter was reprobed with anti-calnexin and anti-β-tubulin antibodies to provide recovery standards for membranes and cytosol, respectively. GBF1-GFP and endogenous GBF1 are predominantly in the cytosolic fraction in control cells and in nocodazole-treated cells (lanes 3 and 9). In contrast, GBF1-GFP and endogenous GBF1 are recovered with membranes in BFA-treated cells (lane 5). Bars represent 16 μm.

cycles rapidly on and off membranes and that the cycling is linked to the catalytic activity of GBF1. Our data are consistent with a model in which GBF1 activates a single molecule of ARF and then dissociates from the ARF and the membrane. The activated ARF remains on the membrane where it facilitates effector functions, including COP I recruitment.

COP I in traffic

COP I and ARF function is required at multiple stages of the early secretory pathway. Experimental evidence indicates that COP I is required to remodel membrane intermediates (called VTCs) generated in the vicinity of ER exit sites into transport competent structures. Specifically, when COP I binding to membranes is inhibited (by expression of a dominant negative GBF1, expression of dominant negative ARF mutants, or BFA treatment), cargo proteins and resident Golgi proteins fail to be transported from the ER to the Golgi (9,22,31). Continuous COP I function is required on VTCs for cargo to move toward the Golgi. This is supported by the finding that microinjection of COP I-specific antibodies that stabilize the association of COP I with membranes arrests VTCs at a peri-Golgi stage (32–34).

Association of COP I with membranes results from rapid cycles of COP I association and dissociation (15,16). The transient nature of COP I binding implies that COP I must be continuously recruited from the cytosol. COP I recruitment is mediated by active ARF. ARF residency on the membrane is also short (15,16), indicating that the ARF-activating machinery, i.e. the GEFs, must be present on all membranes that are COP I coated.

GBF1 cycling between membranes and cytosol

The molecular mechanisms that facilitate membrane association of ARF GEF are unknown. Here, we report on the behavior of GBF1. We used GFP-tagged GBF1, and based on its correct localization and fractionation properties, we propose that it reflects the behavior of endogenous GBF1. Fluorescence recovery after photobleaching imaging shows that GBF1-GFP rapidly ($t_{1/2}$ is approximately 17 ± 1 seconds) exchanges between membranes and the cytosol. GBF1 cycling appears faster than that of ARF (FRAP $t_{1/2}$ is approximately 24 ± 2.7 seconds) under the same conditions used in our studies. This suggests that GBF1 and ARF dissociate from membranes independently of each other and that ARF–GTP remains on membrane after GBF1 dissociates. Our findings are consistent with studies showing that the exchange of GDP for GTP strengthens ARF association with the membrane (5,28) and that GTPase-deficient mutants of ARF persist on membranes (14,35). Activated GTP-bound ARF directly binds to coatomer (36,37) and recruits it to membranes. The faster cycling kinetics of GBF1 suggests that GBF1 does not participate in coatomer recruitment by ARF–GTP. GBF1 behavior is distinct from that of ARF-GAP1, which appears to dissociate from membranes concomitantly with ARF1 (15).

Influence of the GDP/GTP status of ARF on GBF1 cycling

We hypothesized that GBF1 cycling might be influenced by binding to specific proteins. GBF1 interacts with its substrate, ARF, and we explored whether ARF binding regulates GBF1 association with membranes. We present three lines of evidence that GBF1 is stabilized on membranes when complexed with ARF–GDP and is released from both ARF and membranes after it catalyzes GDP displacement and ARF binds GTP.

First, a GBF1 mutant (E794K) cycles slower and remains on membranes longer (FRAP $t_{1/2}$ is approximately 53 ± 12.2 seconds) than wild-type GBF1 (FRAP $t_{1/2}$ is approximately 17 ± 1 seconds). E794K binds ARF–GDP but does not facilitate GDP displacement. Structural information on soluble ARF–GDP, ARF–GTP and complexes of ARF–GDP–Sec7d suggests a sequential progression of molecular rearrangements that leads to GDP expulsion (21,38–40). The initial interaction between the ARF–GDP and the Sec7 domain of the GEF occurs through the switch I region of ARF and a hydrophobic groove formed by the Sec7 domain. The subsequent repositioning of the inter-switch region facilitates the rearrangements of switch II domain within ARF. This positions the GDP moiety in the proximity of the 'glutamic finger' of the Sec7 domain and leads to the displacement of the nucleotide. In E794K, the 'glutamic finger' is replaced with lysine and E794K does not catalyze GDP displacement.

Second, GBF1 remains on membranes longer (FRAP $t_{1/2}$ is approximately 45 ± 5.7 seconds) in cells expressing the T31N mutant of ARF1. T31N has decreased affinity for GTP and is expected to remain in an 'empty' state longer than wild-type ARF. The longer residency time of GBF1 in T31N-expressing cells suggests that the displacement of GDP is insufficient for GBF1 dissociation. It implies that GBF1 dissociation is facilitated by the subsequent binding of GTP by the 'empty' ARF.

Third, GBF1 remains associated with membranes in cells treated with BFA. Brefeldin A inactivates GEFs by forming a ternary complex with ARF–GDP and the GEF (41–43). GBF1 was initially described as BFA resistant, because it was recovered as a factor that confers BFA resistance to mammalian cells (10). However, multiple lines of evidence suggest that GBF1 may be a BFA target. Specifically, overexpression of BFA-sensitive GEFs has been shown to protect cells against BFA (42,44), presumably by sequestering the drug. In addition, the yeast GBF1 homologs Gea1/2p are BFA sensitive (42,45,46). Furthermore, GBF1 mediates COP I recruitment at the ER–Golgi interface (9), and COP I recruitment to ER–Golgi interface membranes is BFA sensitive. Our FRAP findings are consistent with GBF1 being trapped in a BFA–ARF–GDP

complex that is immobilized on the membrane. The data suggest that GBF1 is a BFA-sensitive GEF and a cellular BFA target. While this article was in preparation, similar results showing BFA sensitivity of GBF1 were reported (47).

Our findings lead us to propose a model (Figure 6) for GBF1 cycling. We suggest that GBF1 and ARF–GDP associate with membranes independently. The identity of the membrane 'receptor' for GBF1 is unknown. GBF1 (or its yeast Gea1/2 homolog) has been shown to interact directly with p115 (29), hGmh1 (13,48) and Drs2 (13,48), but none of these interactions are required for GBF1 association with membranes. The mechanisms that facilitate association of ARF–GDP with membranes also appear complex. ADP-ribosylation factor–GDP has been shown to associate with membranes prior to GDP/GTP exchange by binding to p23, a member of the p24 family of proteins (24,49). Recent findings suggest that ARF also binds to ER–Golgi SNAREs (52). The relative importance of the p24 and the SNARE proteins to membrane recruitment of ARF–GDP remains to be elucidated.

Once membrane associated, GBF1 and ARF–GDP interact to form a complex that is stabilized on membranes. Presumably, the complex is stabilized by binding to spatially restricted membrane proteins or macromolecular complexes. Theoretically, stabilization may involve binding to all or some of the proteins known to interact with GBF1 and ARF–GDP.

The GBF1–ARF–GDP complex persists till the GEF activity of GBF1 causes GDP/GTP exchange on ARF and allows GTP binding to ARF. Conformational changes associated with GTP binding are likely to result in the dissociation of ARF from GBF1. This is either concurrent with or is followed by GBF1 dissociation from membranes. Our findings suggest that GBF1 dissociates into the cytosol after catalyzing GDP/GTP exchange on a single ARF molecule. ADP-ribosylation factor–GTP persists on the membrane after GBF1 dissociates and interacts with its effectors.

Materials and Methods

Antibodies, reagents and plasmids

Rabbit polyclonal anti-GBF1 antibodies were described previously (29). The following commercially available antibodies were used: polyclonal anti-calnexin from Stressgen Biotechnologies (Victoria, BC, Canada), monoclonal anti-β-tubulin from Upstate (Lake Placid, NY, USA), monoclonal anti-HA from Santa Cruz Biotechnology (Santa Cruz, CA, USA), polyclonal anti-GFP from Abcam (Cambridge, MA, USA). Secondary antibodies conjugated with HRP, Alexa 488 or Alexa 594, were from Molecular Probes (Eugene, OR, USA). Brefeldin A and Nocodazole were from Sigma-Aldrich (St Louis, MO, USA).

The GBF1 cDNA used in this study has been described (9). Construct encoding GFP-tagged wild-type GBF1 was constructed by subcloning GBF1 into the pEGFP vector using *Xho*I and *Xma*I restriction enzymes. This results in a GFP extension at the N-terminus of GBF1. The E794K-GFP construct has been described previously (MBC paper). Constructs

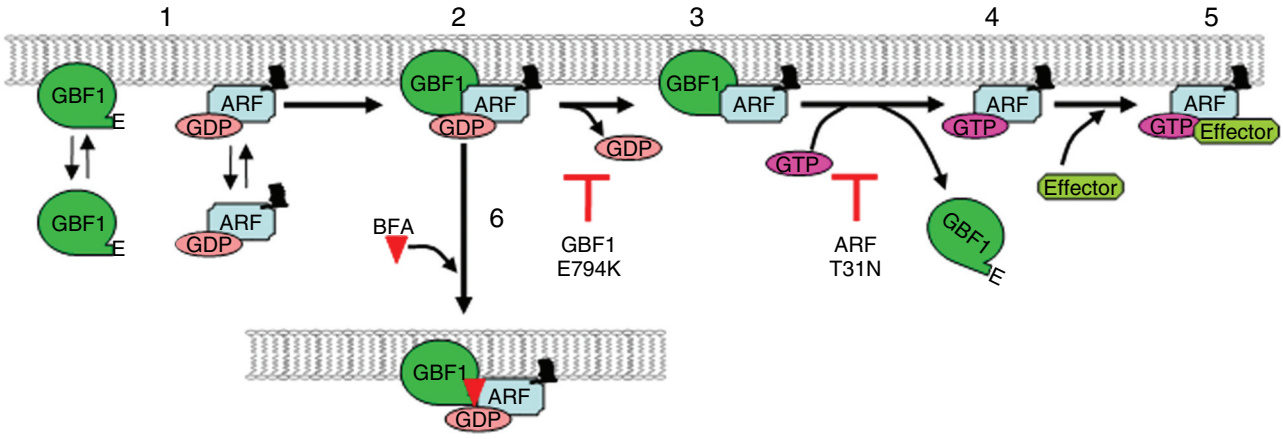

Figure 6: Model for GBF1 cycling at the membrane. GBF1 and ADP-ribosylation factor (ARF)–GDP associate with the membrane independently of each other (step 1). Once on the membrane, the proteins interact and GBF1 initiates GDP displacement from ARF (step 2). A complex of GBF1 and an 'empty' ARF remains on the membrane (step 3) till ARF binds GTP (step 4). GTP binding provides the trigger for complex dissociation, and GBF1 is released from membranes, but ARF–GTP remains on membranes. It then interacts with effectors (step 5) to facilitate COP I recruitment. GBF1 cycling is inhibited by Brefeldin A (BFA). We propose that BFA forms a trimeric complex with GBF1 and ARF–GDP (step 6) and inhibits GDP displacement. This prevents GTP binding to the ARF, and thus prevents conformational changes in ARF that normally lead to its dissociation from GBF1. The complex remains membrane bound presumably associated with the proteins or the macromolecular complexes that normally facilitate its membrane association. The E794K mutant of GBF1 exhibits prolonged membrane association. We propose that E794K binds to ARF–GDP, but does not catalyze GDP displacement. Thus, it blocks GTP binding to ARF (step 4) and prevents conformational changes in ARF that normally lead to its dissociation from GBF1. GBF1 exhibits prolonged membrane association in cells expressing the T31N mutant of ARF. We propose that GBF1 binds ARF-T31N mutant and catalyzes GDP expulsion (step 3). However, ARF-T31N has low affinity for GTP, and this reduces GTP binding and prevents conformational changes in ARF that normally lead to its dissociation from GBF1.

encoding ARF1-HA, ARF1-T31N-HA and ARF1-Q71I-HA were a gift from Dr Julie Donaldson, NIH.

Cell culture and transfection

HeLa cells were used in all experiments. Cells were grown in Dulbecco's modified Eagle's medium with glucose and glutamine (Mediatech, Comprehensive Cancer Center of the University of Alabama at Birmingham), supplemented with 10% fetal bovine serum (Life Technologies, Grand Island, NY, USA), 100 IU/mL penicillin and 100 mg/mL streptomycin (Invitrogen, Grand Island, NY, USA) and 1 mM sodium pyruvate. Cells were grown at 37 °C in 5% CO_2 atmosphere incubator.

Cells were grown on coverslips in 6-well dishes till approximately 70% confluence and were transfected using the Mirus TransIT-LT1 Transfection Reagent (Mirus Bio, Madison, WI, USA), according to the manufacturer's instructions. In some experiments, two plasmids were mixed (1 : 1 ratio) and used for transfection.

Immunofluorescence and live cell imaging

For static immunofluorescence, cells 16 h post-transfection were washed in phosphate-buffered saline (PBS), fixed in 3% paraformaldehyde for 10 min and quenched with 10 mM ammonium chloride. Cells were permeabilized with 0.1% Triton-X-100 in PBS. The coverslips were then washed with PBS and blocked in PBS, 2.5% goat serum, 0.2% Tween-20 for 5 min followed by blocking in PBS, 0.4% fish skin gelatin and 0.2% Tween-20. Cells were incubated with primary antibody for 1 h at room temperature. Coverslips were washed with PBS, 0.2% Tween-20 and incubated with secondary antibodies for 45 min. Coverslips were washed as described above and mounted on slides in 9 : 1 glycerol/PBS with 0.1% *p*-phenylenediamine (Sigma-Aldrich).

Fluorescence patterns were visualized with a Leitz Orthoplan microscope with epifluorescence and Hoffman Modulation Contrast optics from Chroma Technology (Brattleboro, VT, USA). Optical sections were captured with a CCD high-resolution camera from Roper Scientific (Tucson, AZ, USA) equipped with a camera/computer interface. Images were analyzed with a power Mac using IPLab Spectrum software (Scanalytics, Fairfax, VA, USA).

For live cell FRAP imaging, cells were grown in 35-mm glass-bottom culture dishes (Warner Instruments, Hamden, CT, USA) for 16 h after transfection. During the imaging, dishes were placed on thermostage with temperatures ranging between 36 and 37 °C. For imaging experiments, cell culture medium was buffered with 25 mM HEPES, pH 7.4. Imaging acquisition was with the 100X oil 1.4 NA objective of a Leica DMIRBE-inverted epifluorescence microscope outfitted with Leica TCS NT Laser confocal optics (Leica Microsystems, Bannockburn, IL, USA). For FRAP, a 488-nm high-intensity argon laser beam was setup to photobleach a 2-μm diameter spot within a cell for 2–5 seconds at high intensity. Postbleach images were obtained every 7 seconds with a laser set on one directional scan at speed: slow 2. Each round of scanning took 3 seconds in the 1024 × 1024 format. Every image is an average of two frames. Images were analyzed with a power Mac using IPLab Spectrum software (Scanalytics). The fluorescence recovery at each time-point was plotted using the following equation: $I\ (\%) = (R1/R2) \times 100/(R1/R2)^{o}$, where $I\ (\%)$ is the intensity of recovery; R1 fluorescence intensity in the bleached region of a cell; R2 fluorescence intensity in the unbleached region of a cell; R1/R2 ratio of fluorescence intensity in the bleached and unbleached regions of the same cell at each time-point; and $(R1/R2)^{o}$ ratio of fluorescence intensity in the bleached and unbleached regions of the same cell in prebleached cell.

The half-times for fluorescence recovery were calculated using the following equation: $t_{1/2}\ (\text{second}) = [(F_\infty - F_0)/2] + F_0$, where F_∞ is the fluorescence intensity in the bleached region after full recovery and F_0 the fluorescence intensity in the bleached region immediately after the bleach.

For each quantitation, the number of cells imaged is indicated by *n*. Imaging was performed on cells, from at least five to six independent transfections. Graphs were obtained by averaging FRAP values, and SDEV were calculated using Excel software. In some experiments, cells were incubated with 5 μg/mL BFA for 30 min before being processed for static immunofluorescence or live imaging. In some experiments, cells were first incubated with 1 μg/mL of nocodazole for 30 min, and then with 5 μg/mL BFA for 30 min. Cells were then processed for static immunofluorescence or live imaging.

Cell fractionation

Cells were washed with PBS and disrupted in 300 μL of homogenization buffer (50 mM HEPES–KOH, pH 7.5, 100 mM KCl, 1 mM $MgCl_2$, 1 mM DTT) containing protease inhibitors by repeated passage through a 27G needle. The homogenate was centrifuged at 1000 × g for 15 min at 4 °C in a microcentrifuge to remove unbroken cells and nuclei. The postnuclear supernatant was centrifuged in an ultracentrifuge at 100,000 × g for 60 min at 4 °C in a Beckman TLA 100.2 rotor. The supernatant fraction was designated cytosol fraction, and the pellet was rinsed once with homogenization buffer and recentrifuged under the same conditions. The resulting pellet was solubilized in RIPA buffer with protease inhibitors and designated membrane fraction. Fractions containing the same volume of original cells were analyzed by 8% SDS–PAGE. Following SDS–PAGE, proteins were transferred to NitroPure nitrocellulose (NC) membrane (Micron Separations, Westborough, MA, USA), and the membrane subjected to immunoblotting as previously described (50). The same NC was cut into three sections and probed with anti-GBF1, anticalnexin and anti-β-tubulin antibodies. The blots were scanned and the density of bands was quantitated using LabWorks software. The relative intensity of GBF1 bands corrected for intensity of calnexin and β-tubulin bands was calculated.

In some experiments, cells were incubated with 5 μg/mL BFA for 30 min, or with 1 μg/mL of nocodazole for 30 min before fractionation.

Acknowledgments

We thank Albert Tousson at UAB Imaging Core for help with live imaging. We thank Dr J. Lippincott-Schwartz for providing the ARF1-GFP construct and Dr Julie Donaldson for providing the wild-type and mutant ARF1 constructs. We thank Drs Richard Kahn, Pierre Chardin, Bruno Antonny, Cathy Jackson and Sandy Schmid for critically reading the manuscript and helpful comments and advice.

References

1. Barlowe C. Traffic COPs of the early secretory pathway. Traffic 2000; 1:371–377.
2. Nie Z, Hirsch DS, Randazzo PA. Arf and its many interactors. Curr Opin Cell Biol 2003;15:396–404.
3. Donaldson JG, Jackson CL. Regulators and effectors of the ARF GTPases. Curr Opin Cell Biol 2000;12:475–482.
4. Lippincott-Schwartz J, Cole NB, Donaldson JG. Building a secretory apparatus: role of ARF1/COPI in Golgi biogenesis and maintenance. Histochem Cell Biol 1998;109:449–462.
5. Donaldson JG, Finazzi D, Klausner RD. Brefeldin A inhibits Golgi membrane-catalysed exchange of guanine nucleotide onto ARF protein. Nature 1992;360:350–352.
6. Boman AL, Zhang C, Zhu X, Kahn RA. A family of ADP-ribosylation factor effectors that can alter membrane transport through the trans-Golgi. Mol Biol Cell 2000;11:1241–1255.
7. Jackson CL, Casanova JE. Turning on ARF: the Sec7 family of guanine-nucleotide-exchange factors. Trends Cell Biol 2000;10:60–67.
8. Cox R, Mason-Gamer RJ, Jackson CL, Segev N. Phylogenetic analysis of Sec7-domain-containing Arf nucleotide exchangers. Mol Biol Cell 2004;15:1487–1505.

9. Garcia-Mata R, Szul T, Alvarez C, Sztul E. ADP-ribosylation factor/COPI-dependent events at the endoplasmic reticulum–Golgi interface are regulated by the guanine nucleotide exchange factor GBF1. Mol Biol Cell 2003;14:2250–2261.
10. Claude A, Zhao BP, Kuziemsky CE, Dahan S, Berger SJ, Yan JP, Sullivan EM, Melancon P. GBF1: a novel Golgi-associated BFA-resistant guanine nucleotide exchange factor that displays specificity for ADP-ribosylation factor 5. J Cell Biol 1999;146:71–84.
11. Zhao X, Lasell TK, Melancon P. Localization of large ADP-ribosylation factor-guanine nucleotide exchange factors to different Golgi compartments: evidence for distinct functions in protein traffic. Mol Biol Cell 2002;13:119–133.
12. Kawamoto K, Yoshida Y, Tamaki H, Torii S, Shinotsuka C, Yamashina S, Nakayama K. GBF1, a guanine nucleotide exchange factor for ADP-ribosylation factors, is localized to the cis-Golgi and involved in membrane association of the COPI coat. Traffic 2002;3:483–495.
13. Chantalat S, Courbeyrette R, Senic-Matuglia F, Jackson CL, Goud B, Peyroche A. A novel Golgi membrane protein is a partner of the ARF exchange factors Gea1p and Gea2p. Mol Biol Cell 2003;14:2357–2371.
14. Vasudevan C, Han W, Tan Y, Nie Y, Li D, Shome K, Watkins SC, Levitan ES, Romero G. The distribution and translocation of the G protein ADP-ribosylation factor 1 in live cells is determined by its GTPase activity. J Cell Sci 1998;111:1277–1285.
15. Elsner M, Hashimoto H, Simpson JC, Cassel D, Nilsson T, Weiss M. Spatiotemporal dynamics of the COPI vesicle machinery. EMBO Rep 2003;4:1000–1004.
16. Presley JF, Ward TH, Pfeifer AC, Siggia ED, Phair RD, Lippincott-Schwartz J. Dissection of COPI and Arf1 dynamics in vivo and role in Golgi membrane transport. Nature 2002;417:187–193.
17. Hammond AT, Glick BS. Dynamics of transitional endoplasmic reticulum sites in vertebrate cells. Mol Biol Cell 2000;11:3013–3030.
18. Storrie B, White J, Rottger S, Stelzer EH, Suganuma T, Nilsson T. Recycling of golgi-resident glycosyltransferases through the ER reveals a novel pathway and provides an explanation for nocodazole-induced Golgi scattering. J Cell Biol 1998;143:1505–1521.
19. Cole NB, Sciaky N, Marotta A, Song J, Lippincott-Schwartz J. Golgi dispersal during microtubule disruption. regeneration of Golgi stacks at peripheral endoplasmic reticulum exit sites. Mol Biol Cell 1996;7:631–650.
20. Ward TH, Polishchuk RS, Caplan S, Hirschberg K, Lippincott-Schwartz J. Maintenance of Golgi structure and function depends on the integrity of ER export. J Cell Biol 2001;155:557–570.
21. Beraud-Dufour S, Robineau S, Chardin P, Paris S, Chabre M, Cherfils J, Antonny B. A glutamic finger in the guanine nucleotide exchange factor ARNO displaces Mg2+ and the beta-phosphate to destabilize GDP on ARF1. EMBO J 1998;17:3651–3659.
22. Peters PJ, Hsu VW, Ooi CE, Finazzi D, Teal SB, Oorschot V, Donaldson JG, Klausner RD. Overexpression of wild-type and mutant ARF1 and ARF6: distinct perturbations of nonoverlapping membrane compartments. J Cell Biol 1995;128:1003–1017.
23. Dascher C, Balch WE. Dominant inhibitory mutants of ARF1 block endoplasmic reticulum to Golgi transport and trigger disassembly of the Golgi apparatus. J Biol Chem 1994;269:1437–1448.
24. Gommel DU, Memon AR, Heiss A, Lottspeich F, Pfannstiel J, Lechner J, Reinhard C, Helms JB, Nickel W, Wieland FT. Recruitment to Golgi membranes of ADP-ribosylation factor 1 is mediated by the cytoplasmic domain of p23. EMBO J 2001;20:6751–6760.
25. Zhang CJ, Rosenwald AG, Willingham MC, Skuntz S, Clark J, Kahn RA. Expression of a dominant allele of human ARF1 inhibits membrane traffic in vivo. J Cell Biol 1994;124:289–300.
26. Antonny B, Huber I, Paris S, Chabre M, Cassel D. Activation of ADP-ribosylation factor 1 GTPase-activating protein by phosphatidylcholine-derived diacylglycerols. J Biol Chem 1997;272:30848–30851.
27. Franco M, Chardin P, Chabre M, Paris S. Myristoylation of ADP-ribosylation factor 1 facilitates nucleotide exchange at physiological Mg2+ levels. J Biol Chem 1995;270:1337–1341.
28. Kahn RA, Randazzo P, Serafini T, Weiss O, Rulka C, Clark J, Amherdt M, Roller P, Orci L, Rothman JE. The amino terminus of ADP-ribosylation factor (ARF) is a critical determinant of ARF activities and is a potent and specific inhibitor of protein transport. J Biol Chem 1992;267:13039–13046.
29. Garcia-Mata R, Sztul E. The membrane-tethering protein p115 interacts with GBF1, an ARF guanine-nucleotide-exchange factor. EMBO Rep 2003;4:320–325.
30. Lippincott-Schwartz J, Yuan LC, Bonifacino JS, Klausner RD. Rapid redistribution of Golgi proteins into the ER in cells treated with brefeldin A: evidence for membrane cycling from Golgi to ER. Cell 1989;56:801–813.
31. Klausner RD, Donaldson JG, Lippincott-Schwartz J. Brefeldin A: insights into the control of membrane traffic and organelle structure. J Cell Biol 1992;116:1071–1080.
32. Pepperkok R, Whitney JA, Gomez M, Kreis TE. COPI vesicles accumulating in the presence of a GTP restricted arf1 mutant are depleted of anterograde and retrograde cargo. J Cell Sci 2000;113:135–144.
33. Scales SJ, Pepperkok R, Kreis TE. Visualization of ER-to-Golgi transport in living cells reveals a sequential mode of action for COPII and COPI. Cell 1997;90:1137–1148.
34. Shima DT, Scales SJ, Kreis TE, Pepperkok R. Segregation of COPI-rich and anterograde-cargo-rich domains in endoplasmic-reticulum-to-Golgi transport complexes. Curr Biol 1999;9:821–824.
35. Elazar Z, Orci L, Ostermann J, Amherdt M, Tanigawa G, Rothman JE. ADP-ribosylation factor and coatomer couple fusion to vesicle budding. J Cell Biol 1994;124:415–424.
36. Zhao L, Helms JB, Brugger B, Harter C, Martoglio B, Graf R, Brunner J, Wieland FT. Direct and GTP-dependent interaction of ADP ribosylation factor 1 with coatomer subunit beta. Proc Natl Acad Sci USA 1997;94:4418–4423.
37. Zhao L, Helms JB, Brunner J, Wieland FT. GTP-dependent binding of ADP-ribosylation factor to coatomer in close proximity to the binding site for dilysine retrieval motifs and p23. J Biol Chem 1999;274:14198–14203.
38. Renault L, Guibert B, Cherfils J. Structural snapshots of the mechanism and inhibition of a guanine nucleotide exchange factor. Nature 2003;426:525–530.
39. Mossessova E, Gulbis JM, Goldberg J. Structure of the guanine nucleotide exchange factor Sec7 domain of human arno and analysis of the interaction with ARF GTPase. Cell 1998;92:415–423.
40. Goldberg J. Structural basis for activation of ARF GTPase: mechanisms of guanine nucleotide exchange and GTP-myristoyl switching. Cell 1998;95:237–248.
41. Mossessova E, Corpina RA, Goldberg J. Crystal structure of ARF1*-Sec7 complexed with Brefeldin A and its implications for the guanine nucleotide exchange mechanism. Mol Cell 2003;12:1403–1411.
42. Peyroche A, Antonny B, Robineau S, Acker J, Cherfils J, Jackson CL. Brefeldin A acts to stabilize an abortive ARF-GDP-Sec7 domain protein complex: involvement of specific residues of the Sec7 domain. Mol Cell 1999;3:275–285.
43. Robineau S, Chabre M, Antonny B. Binding site of brefeldin A at the interface between the small G protein ADP-ribosylation factor 1 (ARF1) and the nucleotide-exchange factor Sec7 domain. Proc Natl Acad Sci USA 2000;97:9913–9918.
44. Shinotsuka C, Yoshida Y, Kawamoto K, Takatsu H, Nakayama K. Overexpression of an ADP-ribosylation factor-guanine nucleotide exchange factor, BIG2, uncouples brefeldin A-induced adaptor protein-1 coat dissociation and membrane tubulation. J Biol Chem 2002;277:9468–9473.
45. Peyroche A, Courbeyrette R, Rambourg A, Jackson CL. The ARF exchange factors Gea1p and Gea2p regulate Golgi structure and function in yeast. J Cell Sci 2001;114:2241–2253.
46. Peyroche A, Paris S, Jackson CL. Nucleotide exchange on ARF mediated by yeast Gea1 protein. Nature 1996;384:479–481.

47. Niu TK, Pfeifer AC, Lippincott-Schwartz J, Jackson CL. Dynamics of GBF1, a Brefeldin A-sensitive Arf1 exchange factor at the Golgi. Mol Biol Cell 2005;16:1213–1222.
48. Chantalat S, Park SK, Hua Z, Liu K, Gobin R, Peyroche A, Rambourg A, Graham TR, Jackson CL. The Arf activator Gea2p and the P-type ATPase Drs2p interact at the Golgi in *Saccharomyces cerevisiae*. J Cell Sci 2004;117:711–722.
49. Lavoie C, Paiement J, Dominguez M, Roy L, Dahan S, Gushue JN, Bergeron JJ. Roles for alpha(2)p24 and COPI in endoplasmic reticulum cargo exit site formation. J Cell Biol 1999;146:285–299.
50. Gao YS, Alvarez C, Nelson DS, Sztul E. Molecular cloning, characterization, and dynamics of rat formiminotransferase cyclodeaminase, a Golgi-associated 58-kDa protein. J Biol Chem 1998; 273:33825–33834.
51. Tanigawa G, Orci L, Amherdt M, Ravazzola M, Helms JB, Rothman JE. Hydrolysis of bound GTP by ARF protein triggers uncoating of Golgi-derived COP-coated vesicles. J cell Biol 1993;123:1365–1371.
52. Honda A, Al-Awar OS, Hay JC, Donaldson JG. Membrin, an ER-Golgi SNARE, is an Arf1 receptor. Mol Biol Cell 2004;15:189a.